DOI 10.2478/ama-2024-0024

SELECTED RESEARCH ISSUES OF PROTOTYPE FLOATING SYSTEMS

Agnieszka DEREWOŃKO*, Wiesław KRASOŃ*

*Faculty of Mechanical Engineering, Institute of Mechanics and Computational Engineering, Military University of Technology, Sylwestra Kaliskiego Street 2, 00-908 Warsaw, Poland

agnes.derewonko@gmail.com, wieslaw.krason@wat.edu.pl

received 1 March 2023, revised 1 September 2023, accepted 1 September 2023

Abstract: The paper presents a solution that can be used as a temporary supplement to the existing infrastructure in cases of natural disasters, during structure or bridge repair, in military applications and in areas where it is necessary to provide a floating system crossing. The genesis of the proposed structure and its development, as well as examples of applications of the basic module, referred to as the river module – the floating cassette with the pneumatic pontoon – are presented. The original solutions, such as the bow–stern modules, designed using modern, light and durable materials acting as deflectors, are also described. Examples of the use of floating structures composed of identical/repeatable modules–cassettes are shown. The results of experimental tests of two prototype river modules sets are presented as a validation for numerical studies. Selected aspects of static, kinematic and dynamic analyses using finite element and multibody simulations are presented. The numerical simulation of the prototype floating bridge with an assessment of the impact of clearances and an estimation of the kinematic parameters of the floating ribbon with various configurations are described.

Key words: adjustable buoyancy, pneumatic pontoon, field tests, numerical analysis, finite element method, multibody simulation

1. INTRODUCTION

A pontoon bridge is a temporary structure for pedestrian and vehicle travel. A continuous deck is supported by floats. The maximum load it is able to transfer depends on the buoyancy of the floats. Pontoon bridges are used by both the army and civilians [1, 2]. In the military application, pontoon bridges are floating structures, in which the load-bearing elements are rigid, tight, metal tanks. To ensure the possibility of crossing for heavy objects, trucks or tanks, a sufficiently high buoyancy of floats is necessary. In addition, it is essential to provide an adequate number of people and equipment for mounting the floating bridge.

The objects of the discussed type are used mainly by the army for crossing water obstacles [3, 4]. Instances of their deployment are also found in civil applications; for instance, in emergency services and territorial defence units during natural disasters (flooding) for evacuating the population. They can also be used for the needs of local self-governments, among others when the possibility for the use of a fixed bridge becomes excluded owing to damage or destruction.

The unquestionable advantages of the pontoon bridge include its simplicity of construction and the possibility of combining different construction systems, depending on the type of water crossing. This solution allows the assembly of a pontoon bridge in various configurations [5].

The other advantage of the pontoon bridge is the possibility of using it regardless of the depth and length of the water crossing and various terrain conditions. However, the disadvantage that is associated with it is the large volume of floats required, and therefore, the need for a large storage area and a number of transport vehicles. The solution of the floating system presented here can help avoid a large part of these inconveniences.

The concept and development of the proposed mobile pontoon bridge with adjustable buoyancy have been presented in Refs. [6–9]. This type of construction results in the phenomenon that the deflection of the ribbon is partially offset by the buoyancy of water during the crossing of heavy objects such as tanks (Fig. 1).

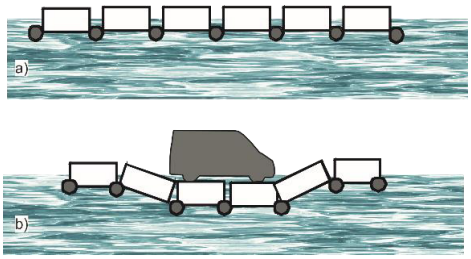

Fig. 1. Scheme of the deformation stages of a ribbon floating bridge: (a) unloaded, (b) loaded

The methodology of determining the buoyancy of a single module using the pneumatic carrier object (PCO) as well as the analysis of the stability of a single module has been presented in several previous papers [7–9]. The theoretical foundations of the vibration analysis of a multicomponent structure can be found in the studies of Xiang et al. [10], Liu [11] and Shao et al. [12]. Fragments of the kinematic and dynamic analyses carried out for the presented structure are illustrated in the studies of Derewońko et al. [7] and Krasoń and Sławek [8]. The experimental tests used to determine the strength of the complete bridge spans are discussed in Melcer's study [13], with this author having discussed selected aspects of the experimental strength tests of the prototype floating cassettes and innovative rod joints used to connect

DOI 10.2478/ama-2024-0024

cassette modules into a floating ribbon [9, 14–16]. The mobile pontoon bridge was transported on trailers of standard dimensions and installed in the desired location [9].

The floating systems studied in this work are composed of repeatable modules. Such an object is considered as a multiunit system with movable joints between the modules with assembly clearances. Experimental tests of complex, large-sized structures with clearance are difficult and expensive. Theoretical–analytical methods have some limitations due to geometrical nonlinearities determined by clearances. Therefore, simulation methods for tests using numerical analyses of multipart systems with clearances have been gradually improved. A typical approach to the research of complex multibody structures is multistage analysis as well as the analysis of selected parts of the complex structure. The original methodology of modelling as well as selected aspects of field tests, numerical finite element (FE) and multibody analysis of floating systems with constructional clearances are discussed in detail in the example of these prototype structures.

2. MOBILE PONTOON BRIDGE PROTOTYPE

The mobile pontoon bridge is classified as a "ribbon" floating bridge [7–9]. In terms of the static scheme, it is a continuous beam resting on a springy base. A scheme of the bridge without loading is shown in Fig. 1a. Deformation of the bridge caused by the force corresponding to the total weight (dead weight + load) of the conveyed vehicle is shown in Fig. 1b.

2.1. Design assumptions

A completed section of the mobile pontoon bridge is a river module performing a triple function: floating support, supporting structure and roadway. Requirements for this type of structure for military objects with the given parameters, e.g. MLC 70 class for wheeled vehicles and MLC 80 for tracked vehicles, were included in military standards, e.g. in the Polish NO-54-A203 [17] or in a trilateral agreement on a military bridge and crossing equipment concluded by the Federal Republic of Germany, the UK and the USA [3]. The MLC abbreviation is understood as a designation of a facility military load class in accordance with the NATO STANAG 2021 standardisation [4].

The mobile pontoon bridge can be developed by assembling individual modules in a desired configuration, the exemplary models of which, including models of vehicles being conveyed, are shown in Fig. 2.

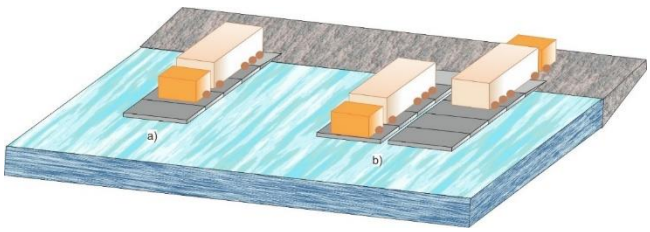

Fig. 2. Examples of a ribbon: **(a)** single, **(b)** double

Initial work on the design of the cassette pontoon bridge included simulation of a single-ribbon model composed of three modules connected by mechanical locks under a moving load [9]. The vehicle was assumed to have the following characteristics, that is to say a weight of 4,000 kg, movement at a speed of 20 km/h along the track and in the direction presented in Fig. 3a, and the supporting of its weight by four wheels (Fig. 3b). The distance between the single tracks corresponded to the wheel spacing of the moving object.

When a vehicle with an assumed wheelbase exceeding the width of one module (i.e. an assumed wheelbase having a width greater than 2 m) was moving, the front wheels pressed on the modules, and differently from the pressing observed in the case of the rear wheels, thus causing deformations of different parts of the road surface in the adjacent modules. In Fig. 3a, a tracing of the wheels during the whole simulation of the vehicle movement is marked. On the other hand, Fig. 3b depicts the wheel tracing for the selected shorter-ride time interval.

The deformation of the cassette roadway surface in the selected time step under the pair of wheels (Sections 1 and 2 in Fig. 3a) in the direction of the repetitive module width is symbolically shown in Fig. 3c. The image of deformations of the roadway surface along the set of modules (in the vehicle-movement direction) under the front and rear wheels for the same time step is shown in the same way in Fig. 3d. This section is marked in Fig. 3a with the numbers 2 and 3.

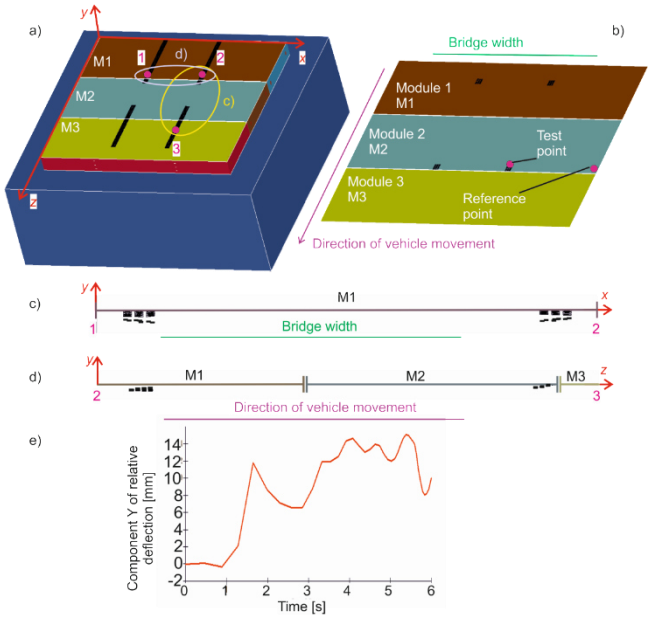

Fig. 3. Single-ribbon model: (a) vehicle motion track, (b) displacement registration points, (c) roadway deformation in the module width direction (O–X), (d) roadway deformation in the vehicle-movement direction (O–Z), (e) difference in vertical relative displacements (O–Y) determined in the test point and reference point (at module 2) as function of time

The relative deflection of the road surface caused by the wheel load, presented in the form of a graph in Fig. 3e, was obtained by referring the vertical displacement value Y of the node located on the roadway under the centre of a single wheel to the appropriate displacement of the node lying on the edge of the roadway.

DOI 10.2478/ama-2024-0024

2.2. River and bow–stern modules of a floating system

The main structural element of a single module is a closed metal cassette. Its required strength was ensured by the upper part, i.e. the roadway (Fig. 4a). The cassette is also a container for a PCO, constituting its basic protection, especially during transport, loading–unloading and launching–taking from water operations. In the opened position, the elastic pontoon (PCO) is folded inside the cassette (Fig. 4b).

In the lower part of the cassette, a movable bottom with a metal-composite structure was mounted. It can move downwardly under the pressure of the air-filled PCO. The return movement of the bottom was enabled by a set of 10 spring-telescopic mechanisms [6, 18, 19] placed symmetrically on both sides of the cassette (Fig. 4b), whereas the initial tension of the springs constituting the element of the telescope-spring mechanism allowed for tight closing of the cassette.

In the original version of the module structure, while opening the module, the deflector plate automatically extended from the side of the module stem (Fig. 4b) [9]. Such a construction of the cassette ensured the required strength and buoyancy, which allowed modules to be connected on water before filling the PCO with compressed air.

Fig. 4. Single prototype module – cassette with PCO: (a) in the closed position of the bottom plate – PCO without compressed air, (b) in the opened position of the bottom plate with PCO filled with compressed air. Designations: 1 – horizontal rod joints, 2 – cassette with roadway, 3 – vertical rod joints, 4 – module stem-deflector, 5 – bottom plate, 6 – elastic pontoon, and 7 – single telescopic mechanism

The cassettes were coupled by a set of mechanical locks [9, 14–16], which were vertical and horizontal rod joints (Fig. 4a). In addition, the connection of the cassettes on the road surface was carried out by the rotating arms [9]. The use of such side connections allowed for the immediate compilation of temporary crossings in the form of single-ribbon bridges of various lengths.

The bow–stern modules were unusual and innovative elements of the floating system equipment. Mounted at the bow and stern, they acted as deflectors, providing a streamlined shape, which reduced the resistance of the unit movement on the water. At the same time, they ensured user safety and increased the operational space of the system, which can be understood as an advantage in terms of facilitation of deck accessibility for the crew. From the side of the pressing water, the module surface was specially shaped (Fig. 5), which provided the proper direction of water streams flowing around the set of modules.

The use of unusual materials and innovative structures allowed for increasing the buoyancy of the entire set. A single bow–stern module in the basic version with a load capacity of 18 kN could be folded into a set of two cassettes connected side by side [8, 9]. The structural solution of this sub-assembly allowed for the connection to the bow or the stern of the modules and determined the increase in the width of the module set deck by 1.2 m on each side. The connection with cassettes was made using the bow–stern horizontal rod joints (Fig. 5) that carried the main loads acting on those components. The top surface of the bow–stern module was inclined towards the cassette roadway, which formed an additional protection for the users of the floating object. The structure of the module enabled the assembly of protective barriers for the service crew.

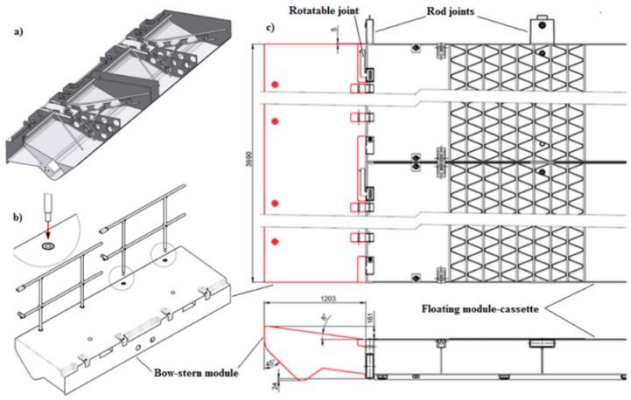

Fig. 5. Bow–stern modules: (a) internal space of module, (b) bow–stern module with protective barrier, (c) views of the floating system with two cassettes-river modules, joints and bow–stern overlays

The deflector designed in the unusual version of the cassette, used to properly direct the flow of water streams after opening the cassettes and filling the PCO, as well as for protecting the PCO from damage, was replaced with a system of expandable shutters (Fig. 6). This system was mainly used to reduce water resistance forces and eliminate ballistic threats. Due to the self-retracting mechanism, it was also possible to automatically roll up and fold the shutter system together with the movement of the bottom of the cassette.

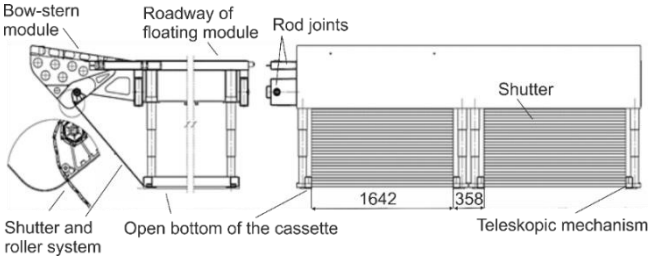

Fig. 6. Structure of roller shutter system in the basic version, mounted unilaterally on two river modules (in two views)

2.3. Example of mobile floating sets of individual modules as objects of research

The single floating module can also be used in the structure of a mobile floating ferry (Fig. 7) with its own roadway, consisting of 6 or 12 modules in various configurations [9]. Depending on the

required load space and load capacity, it was possible to combine different ferry variants.

The proposed solution allowed for building ferries in the 1 × 6 longitudinal configuration with a cargo space of 12 m × 6.3 m and a load capacity up to 480 kN and a parallel system 2 × 3 with a loading area of 12.7 m × 6 m and a load capacity up to 480 kN (Fig. 7).

The basic version is a fragment of a double ribbon with a length of 6 modules, which was a variant of the platform 2 × 6, i.e. a combination of 12 cassettes connected in 2 rows of 6 pieces each, with a loading space equal to 12.7 m × 12 m and a load capacity up to 960 kN. Additionally, with the use of two bow–stern modules, the operational space of each variant of a ferry increased the object roadway by 2.4 m.

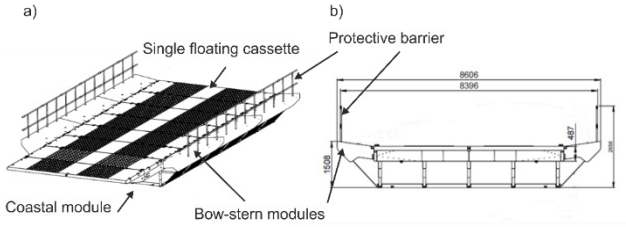

Fig. 7. Mobile floating platform in the 1 × 6 variant with the bow–stern modules and coastal modules in two views: (a) diagonal, (b) forehead view

3. EXPERIMENTAL TESTS OF TWO PROTOTYPE RIVER MODULES SETS

Experimental load tests of a prototype module were performed [9]. The research was carried out on a single-river module and a set of two connected cassette bridge pontoon modules.

The schedule of experimental tests of a single module and a set of two connected river modules included:

- an attempt to launch a single module with a closed bottom and register the value of its own immersion;
- the registration and evaluation of the operation of a single module on water in a closed state (without filling PCO with compressed air);
- the registration and evaluation of the process of filling a PCO before launching and after immersion in water;
- an assessment of the buoyancy and stability of the two-module set (after connecting the side locks and in the plane of the cassettes roadway), with the maximum filling of the PCOs;
- the observation and registration of the PCO-emptying process on water – an attempt to close the cassettes in water.

An experimental test of loading a two prototype river modules set, after filling a PCO with air, is shown in Fig. 8.

The test consisted of a sequential loading of the test modules with successive weights of appropriately selected masses of 1,000 kg or 1,600 kg. The maximum load value was 12.2 tonnes. The weights were set using a crane on the roadway of two connected river modules (Fig. 8).

The recording of module motion and the measurement of the set immersion were carried out using high-speed cameras to register the fast-changing phenomena. The results of the experimental test allowed assessment of the values of the changes in the dives, corresponding to the specific external loads, in individual loading sequences. The tests also allowed for the determination of the load corresponding to the critical immersion of the ribbon when the plane of the module roadway was in the water surface plane.

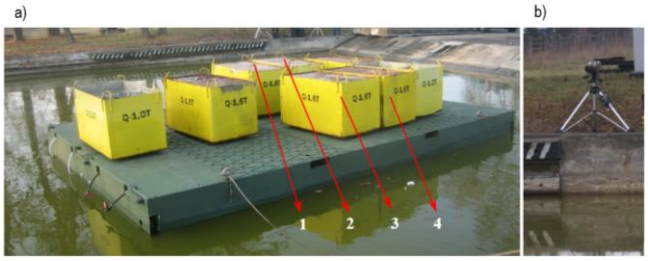

Fig. 8. Experimental load test of a set of two connected modules in WZI S.A. basin: (a) view after adding the last (8th) weight and obtaining the final load of 122 kN and (b) one of the cameras recording the field tests

Due to the limited memory of the cameras used (8 GBit), the recording time at full resolution and recording at 24 frames per second was approximately 4 min (231 s). The cameras were placed in perpendicular directions during the tests (Fig. 8b): one camera recorded the movement of the bow of the prototype pontoon assembly, and the other camera recorded the behaviour of the left side of the assembly. Based on the archived images of each camera, both the heights above the water surface of the centres, respectively the bow and the starboard side, as well as the inclination angles of the pontoon group in the transverse and longitudinal planes, were determined. Based on these results, it was possible to determine the displacements and angles used in the process of tuning the parameters of the numerical models and verifying the calculation results.

Based on the performed tests, it was found that the prototype river modules were characterised by high buoyancy and necessary stability. The tilt angles of the roadway, measured in the direction transverse to the set roadway axis and in the longitudinal direction, do not exceed 5°. Given the prevalence of a total external load of 12.2 kN, the modules' immersion in water was observed, with the result that the so-called "freeboard" was maintained, that is to say, there was a part of the module (measuring about 0.4 m) extending over the water surface (parameter H in Fig. 9). Thus, a large reserve of displacement of the two river modules assembled in such a way in the open configuration was obtained, with the PCO completely filled with air.

The graphs illustrating changes in the height value of the centre point of the right side, roadway and bow centres over the water level as a function of time are presented in Fig. 9a. These charts are a fragment of the full record of the changes in immersion during the sequential load process and correspond to the load phase of the module set with two, three and four weights (1–4 in Fig. 8).

The time interval from 178 s to 131 s corresponded to the load of the module set with four weights with a total weight of 64 kN. The value of the roadway centre height above the water plane varied between 660 mm and 720 mm. The average value of "freeboard" height H measured at the centre point of the roadway from the above range (marked with a square field with a blue background in Fig. 9a) was 690 mm.

The immersion *V* (Fig. 9**b**) of the cassette in the field test was determined according to the relationship:

DOI 10.2478/ama-2024-0024

$$V(t) = 1300 - H(t)\ [\text{mm}] \quad (1)$$

where the value of 1,300 mm is the structural dimension corresponding to the total height of the cassette and H(t) is the height of the "freeboard" measured at various points (Fig. 9b) of the cassette during the field test. The average value of the cassette immersion corresponding to the "freeboard" H = 690 mm was therefore V = 610 mm. This immersion value was used to tune and validate the numerical multibody model of the two cassettes presented in Sections 4 and 5.

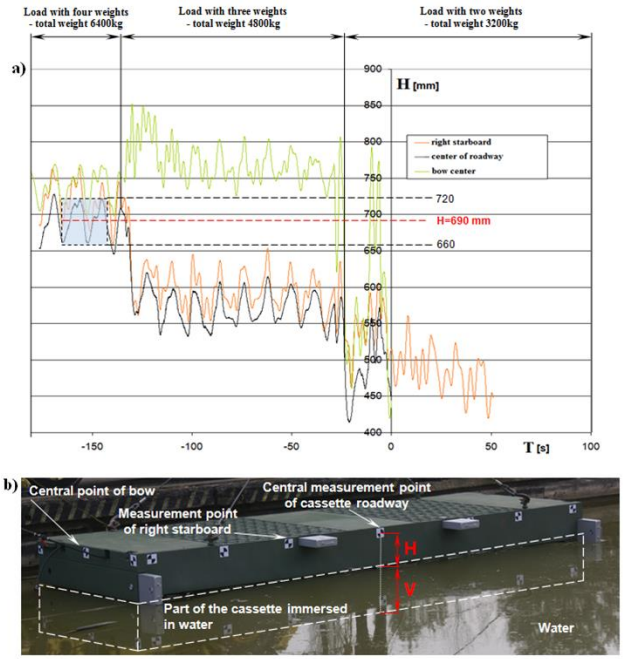

Fig. 9. Selected results of "freeboard" – the H measurement and the idea of immersion determination in a sequential load process during field tests: (a) changes in the value of the right starboard, roadway and bow centre's height over the water surface as a function of time during the loading process,(b) position of measurement points on the cassette and the view with an interpretation of the measurement parameters, H – height of the "freeboard" and the corresponding V – the immersion of the cassette

4. NUMERICAL STUDIES OF FLOATING SETS – VALIDATION TESTS

4.1. Methods of numerical simulations

Multibody system (MBS) and FE simulations were applied to selected aspects of the static, kinematic and dynamic analyses of the prototype floating bridge.

Newton and Euler equations (Newton's 2nd law and theorem related to rigid solid angular momentum change) as a relation (Eq. (2)) are often used to describe rigid body motion in MBS simulations.

$$m\dot{\boldsymbol{v}}_{\mathrm{c}} = \boldsymbol{F};\ \ \dot{\boldsymbol{K}}_{\mathrm{c}} = \boldsymbol{N}_{\mathrm{c}} \quad (2)$$

Angular momentum vector components $\dot{\boldsymbol{K}}_{\mathrm{c}}$ of the analysed object are defined in the following way:

$$\boldsymbol{K}_{\mathbf{c}} = \boldsymbol{J}_{\mathbf{c}}\omega \quad (3)$$

where $\boldsymbol{\omega} = [\omega_\xi\ \omega_\eta\ \omega_\zeta]^T$ and $\boldsymbol{v_c} = [v_{cx}\ v_{cy}\ v_{cz}]^T = [\dot{\boldsymbol{x}}_c\ \dot{\boldsymbol{y}}_c\ \dot{\boldsymbol{z}}_c]^T$ is the generalised velocity of the centre *C* of the mass system.

In such a case, the solid motion equation takes the form (Eq. (4)):

$$\begin{bmatrix} m\boldsymbol{I} & 0 \\ 0 & \boldsymbol{J}_{\mathbf{c}} \end{bmatrix}\begin{bmatrix} \dot{\boldsymbol{v}}_{\mathbf{c}} \\ \dot{\boldsymbol{\omega}} \end{bmatrix} + \begin{bmatrix} 0 \\ \tilde{\boldsymbol{\omega}}\boldsymbol{J}_{\mathbf{c}}\boldsymbol{\omega} \end{bmatrix} = \begin{bmatrix} \boldsymbol{F} \\ \boldsymbol{N}_{\mathbf{c}} \end{bmatrix} \quad (4)$$

where $\mathrm{J_c}$ represents the solid polar moment of inertia and $\mathrm{N_c}$ the moment of external forces (F) in relation to the center of mass C.

In the static FE tests for the developed numerical model of the mobile pontoon bridge with nonlinearities resulting from the contact phenomena and clearances, the analyses were conducted with the use of an iterative calculation algorithm. The algorithm in question is based on the Newton–Raphson scheme [20] and allows the analysis of the systems with a variable stiffness matrix resulting from the equilibrium state determined by equation Q = f(q), where Q represents the vector of external forces and q is a value of displacement corresponding to it.

4.2. Numericl MBS models

The research results were applied to build and validate numerical models of the experimentally tested set of two modules and models of single floating ribbons of various lengths and self-propelled floating platforms. Selected models used in numerical studies of module sets combined into floating platforms and into sections of the bridge ribbon are presented in Fig. 10.

The model shown in Fig. 10a was used in multivariate multibody analyses, in which load tests performed in field conditions were mapped. The model mapped the contact phenomena, friction in the locks joining the modules and a discrete influence of water represented by a set of springs with substitute stiffness determined based on the Winkler model.

Numerical models composed of rigid bodies (MBS models) or deformable bodies, respectively, represented by various FEs in the finite element method (FEM), were used in the verification tests and in the process of tuning the equivalent stiffness values and damping for the floating bridge multibody models. Rigid bodies mapping individual floating modules–cassettes (Figs. 10 and 12) in the MBS or deformable FEM models were connected with each other by means of movable constraints of the cylindrical joint type located in the plane of the bottom of the floating bridge set. The contact surfaces were mapped in the plane of the bridge roadway for the MBS and FEM numerical models considering assembly clearances (in the unloaded state) and appropriately selected structural damping. Spring-dampening elements were attached to the bottom of the models of individual cassettes (Figs. 10 and 12) for modelling the interaction of water with substitute parameters of stiffness (linear Winkler theory) and damping (Fig. 11) selected based on data recorded in field tests with a set of two cassettes (Fig. 10a).

Methods and procedures for determining stiffness and damping in mechanical problems are issues that were presented in scientific publications on modelling and simulation of dynamic problems, e.g. Refs. [8, 9, 21, 22]. The results of experimental tests recorded during field tests with a set of two prototype cassettes (presented in Section 3) were used for this purpose. The

work also used the comparative methodology of matching substitute values of stiffness and damping in numerical models, as explained below.

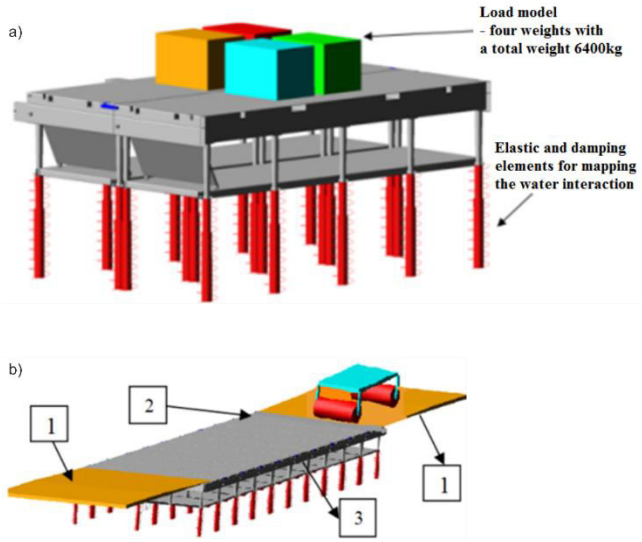

Fig. 10. Numerical rigid models of selected floating objects assembled from prototype modules: (a) multibody model of two floating modules set used in verification tests and for selection of substitute stiffness and damping values, (b) multibody model of single ribbon: 1 – coastal module, 2 – roadway, and 3 – river module

The diagrams of the changes in the maximum immersion of a two river modules set loaded at the same time with four weights as a function of time are shown in Fig. 11a. The average value of the immersion changes, referred to here as displacements of the central point of the cassette roadway and shown in Fig. 11a, was 610 mm. This value (V in Fig. 9b) corresponded to the average value of the "freeboard" height H = 690 mm measured at the central point of the cassette roadway during the field tests, as it is presented in Fig. 9a. A diagram of the change in the contact force in the pivot arm connecting the river modules in the plane of the roadway during the load test simulation is presented in Fig. 11b.

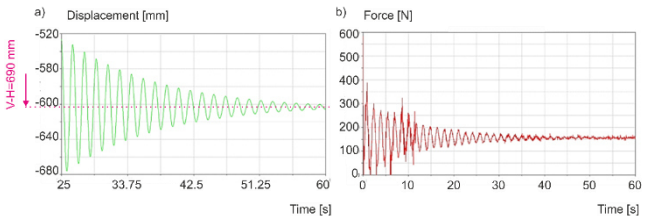

Fig. 11. Graphs of changes in kinematic and static parameters of the set after model's validation: (a) changes of displacements as a function of time, (b) changes of contact forces in the rotating arm connecting river modules during load test simulation

A three-dimensional multibody model of a single ribbon/platform, about 30 m long and 6 m wide (shown in Fig. 10b), was used in numerical studies conducted to ascertain the influence of the moved object's weight and position on kinematic and static parameters of the floating bridge section built of prototype modules connected by side locks.

Multiset numerical studies of the floating platform with coastal modules were carried out. The set was loaded with the weight of the vehicle entering from the coastal module (1 in Fig. 10) and going to the platform external module (2 in Fig. 10) and moving along the platform at a constant speed of 1.5 m/s. In the initial variant P, only the self-weight of the floating structure including coastal modules (about 260 kN) was considered. In variant I, the total vehicle weight was 3.5 tonnes and in variant II, it was 10 tonnes.

5. NUMERICAL SIMULATION OF PROTOTYPE FLOATING BRIDGE

Numerical methods may be used even at the preliminary stage of the tests of the structures (Fig. 2). Due to the nature of the preliminary work, it is often necessary to perform verifying calculations repeatedly.

Multivariant load models, including time-varying models, inertial mapping of moving vehicles (multibody model – Fig. 12) and FE statics loads, were used in multivariant simulations under the influence of the size of clearances and various friction conditions.

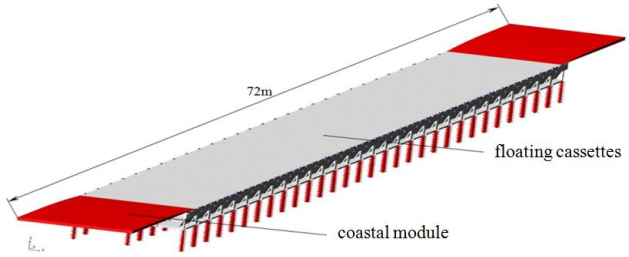

Fig. 12. Rigid body–MBS models of a single-ribbon type bridge for MB dynamics simulation

The model of the bridge section with the coast modules tested with the multibody method in the single-ribbon variant is shown in Fig. 12. The tested floating ribbon was composed of 30 prototype cassettes and two coast ramps. Each ramp was 6 m long and 6.25 m wide, corresponding with the dimensions for the bridge cassettes. Each ramp's mass was 6,000 kg. The end sections of both ramps were articulated with no translation displacement at the edges of the crossing (edge anchoring). The other end of the ramp rested on the roadway of the last mobile pontoon bridge ribbon cassette and was joined with it in a non-movable manner. The other end of the entry ramp was based on the road plate of the extreme cassette and the contact conditions along with the friction ones on the ribbon surface were defined. In the bridge model, three-dimensional connections between the individual cassettes of the set were mapped with the definitions of contact zones and assembly clearances corresponding to the nominal values provided for this type of structure.

In the static FE analysis, the floating ribbon was loaded in half of its length with a stationary lump representing various weights of the tracked vehicles being crossed: 100 kN, 250 kN, 500 kN and 700 kN. The dimensions of the body modelling the chassis of the tracked vehicle and the contour of the track in contact with the ribbon road were defined based on the STANAG standard [4], in accordance to the 50 MLC load class for tracked vehicles. In dynamic simulations, the solids modelling the tracked vehicle were given a constant speed of u = 5 m/s. In this way, the movement of the transported vehicle was modelled in relation to the

DOI 10.2478/ama-2024-0024

road of the ribbon model compiled from the same floating cassettes, as given in Fig. 13. In individual variants of the dynamics analysis, identical weights of the vehicles were defined as in the statics analysis. In each considered variant, only a symmetrical passage along the longitudinal axis of the ribbon was defined (Fig. 13). Submersions and internal forces in the locks of such defined single-ribbon models were analysed.

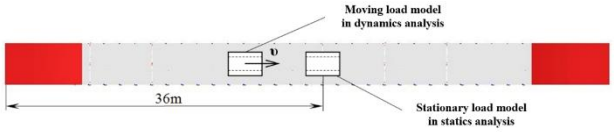

Fig. 13. The single-ribbon type model built from floating modules in the top view with models of stationary loads (statics analysis) and moving loads (dynamic analysis)

The changes in the floating ribbon's submersions recorded in the section corresponding to half the ribbon's length as a function of time during the runs of the vehicle with different weights – 100 kN, 250 kN, 500 kN and 700 kN – are summarised in Fig. 14. The maximum submersion values were determined as the differences in V displacements defining the initial and final positions of the cassette in the cross-section corresponding to half of the length of the floating ribbon in the individual load variants.

The results of the submersion numerically determined in the FE models of the floating ribbon (statics analysis) with results from the multibody tests – dynamic simulations – are compared in Tab. 1.

The maximum vertical displacements determined in the static analysis with FE models of the floating ribbon were greater by 9.9% and 0.9%, respectively, for loads of 250 kN and 500 kN, and lower by 4.2% for a load of 700 kN, than the maximum ribbon draft (submersion) determined in the dynamic analysis for analogous moving loads.

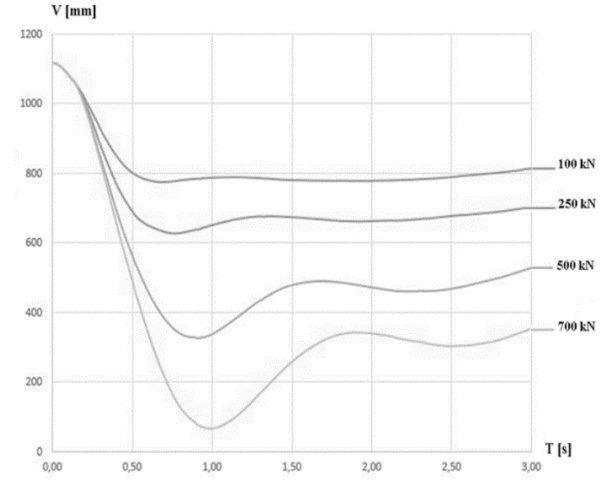

Fig. 14. Results of the MBS analysis: changes in vertical displacements of the cassette recorded in the middle of the ribbon length as a function of time during the runs of vehicle with different weights: 100 kN, 250 kN, 500 kN and 700 kN.

Prototype floating bridges with the maximum displacement (PCO is fully filled with air), in mixed and double ribbon systems, may operate safely in crossings of vehicles with a weight of 1,000 kN (100 MLC according to the NATO classification [4]) moving at a speed of about 5 mps. The allowed load capacity of a single prototype ribbon was 700 kN (70 MLC).

Tab. 1. Comparison of results of numerically determined maximum submersion values in 3D models built of rigid and elastic bodies for various load values according to STANAG 2021 [4]

Load [kN]	Maximum submersion FE static analysis *V* [mm]	Maximum submersion MB dynamic analysis *V* [mm]	Relative differences $\left(\frac{\lvert V_{\max}\rvert - \lvert V_{\min}\rvert}{\lvert V_{\min}\rvert}\right) \cdot 100\%$
250	500	455	9.9
500	687	681	0.9
700	823	858	4.2

6. CONCLUSIONS

The main original achievement of this work is the experimental and numerical research methodology established for testing the strength of multibody systems, which include modular floating systems. The work shows that the methodology can be used to test various floating systems in which, under the influence of moving loads, the assembly clearances change and the main part of them is formed without the clearances, the so-called "compact zone." This part of the modular floating object submerges the most because it absorbs all the loads from the moving object. An additional difficulty in static and dynamic tests of such systems, such as floating bridges, is the strong curvature and variable lengths of the compact zone depending on the weight of the objects being crossed. Moreover, a compact zone understood in this way is created directly under the vehicle being crossed. Its strong curvature results from the selection of clearances only in that part of the bridge that directly absorbs the loads from the vehicles being crossed. If the vehicle moves relative to the longitudinal axis of the floating bridge, the compact zone also moves with it. Correctly representing these phenomena in numerical simulations is a serious scientific challenge.

(1) The original achievements presented in the work are:

- a methodology for selecting substitute parameters – stiffness and damping – describing the multisegment model of the prototype bridge;
- verified based on experimental research, multimember models built of rigid bodies for MB simulation and results of dynamic analysis in models of floating bridges representing real crossing facilities;
- the possibility to determine the MLC classification of different variant floating bridges according to NATO STANAG military load standards, based on results of computer simulations.

(2) A river module with a movable bottom, with adjustable buoyancy, was characterised by a very good ratio of dead weight and usable carrying capacity to the working and transport volume.

(3) The structure in both the prototype and modernised version was tested in terms of strength and functionality. The verification tests of the assumptions, load capacity analyses and safety and strength in various operational states were carried out in laboratory tests and field tests as well as in computer analyses

with the use of advanced simulation techniques. The results obtained by numerical simulation were consistent to the experimental results.

(4) The structural modifications introduced in a single-river module allowed increasing of the range of potential applications of floating systems built on their basis. An increase in the structure susceptibility, as understood in this way, was confirmed. The possibility of building any configurations of ferries or floating bridges was proved.

(5) The bow–stern modules increased the operational space of the crew and the load capacity of the entire system and reduced the resistance of the set movement on water. The additional advantage of using the bow–stern modules was a roller shutter system, which, owing to the inclusion of a pneumatic carrier object filled with compressed air, can function as a ballistic protection as well as a protection against the occurrences of damages of various kinds.

(6) The repeatability of a single module and its ease of transport and operation make it possible to use it in many applications from the crossing of military vehicles (e.g. tanks), through replacement passes for trucks (e.g. providing materials for construction of a permanent bridge), to single-replacement ribbons for flooded roads and footbridges on suddenly enlarged watercourses.

(7) In the future, due to safety and functionality reasons, it is advisable to divide a PCO into at least three, independently assembled, chambers with a less complicated shape and a possibility of individual replacement in case of damage. External, high-strength joints of individual chambers would allow for creation of a coherent, multichamber pneumatic support body. The joints would be resistant to hydrostatic and hydrodynamic forces, external load and deformation of the bridge lines caused by them. The shape of a single chamber, similar to a rectangular prism, would limit the phenomenon of a number of internal tendons forming the walls of a PCO or would even eliminate the necessity for their use.

REFERENCES

1. Leqia He, Chiara Castoro, Angelo Aloisio, Zhiyong Zhang. Dynamic assessment. FE modelling and parametric updating of a butterfly-arch stress-ribbon pedestrian bridge. Struct Infrastruct Eng, 2021;18(7): 1064-1075.
2. Minwoo Chang, Sung Il Seo & Hyung Suk Mun. Running Safety and Behavior Tests for a Scaled-Down Railway Vehicle Crossing a Floating Bridge. KSCE J Civ Eng. 2020;24:1750–1762.
3. Hornbeck B, Kluck J, Connor R. Trilateral Design and Test Code for Military Bridging and Gap-Crossing Equipment. TARDEC BRIDGING 2005. http://www.dtic.mil/dtic/tr/fulltext/u2/a476390.pdf
4. STANAG 2021 Ed.8. Military Load Classification of Bridges, Ferries, Rafts and Vehicles. http://nso.nato.int/nso/nsdd/_CommonList.html]
5. Derewońko A, Krasoń W. Mobile pontoon bridge and floating systems, Special Interest Group A2 (Ports and Maritime) of the World Conference on Transport Research Society (WCTRS). Antwerpia conference proceedings. 3-4 May 2018.
6. EP2251255B1 2013. A sectional pontoon bridge. Military University of Technology.
7. Derewońko A, Kołodziejczyk D, Golczak K, Pneumatic Air Object Application in Design Of Water Crossing. Journal of KONES.2015; 19(4):155-161. DOI: 10.5604/12314005.1138333.
8. Krasoń W, Sławek P. Design and pre-testing of a mobile modular floating platform with adjustable displacement. Mechanik 2017;90(11). DOI: https://doi.org/10.17814/mechanik.2017.11.185
9. Krason W. Selected Problems of the Numerical Capacity Assessment for Floating Systems. Modelling in Engineering 2020: Applied Mechanics. Part of the Advances in Intelligent Systems and Computing book series (AISC, volume 1336), eBook ISBN978-3-030-68455-6. DOI https://doi.org/10.1007/978-3-030-68455-6pp. 168-180
10. Xiang X et al. Viscous damping modelling of floating bridge pontoons with heaving skirt and its impact on bridge girder bending moments. The 36th International Conference on Ocean, Offshore and Arctic Engineering. June 25-30. 2017. Trondheim Norway.
11. Jiachen Liu. Development of Vibration Base Health Monitoring in Bridge. Journal of Physics Conference Series 012021. September 2021. DOI:10.1088/1742-6596/2014/1/012021
12. Yanlin Shao, Xu Xiang, Jianyu Liu. Numerical Investigation of Wave-Frequency Pontoon Responses of a Floating Bridge Based on Model Test Results. Conference: Proceedings of the 38th International Conference on Ocean. Offshore and Arctic Engineering. June 2019. DOI:10.1115/OMAE2019-96545
13. Melcer J. Experimental Testing of a Bridge. Applied Mechanics and Materials. 2013; (486):333-340.
14. Krason W, Popławski A. Numerical research of the cassette bridge joint strength with mapping of stand for experimental tests. Cite as: AIP Conference Proceedings 2078, 020050 (2019). https://doi.org/10.1063/1.5092053, Published Online: 04 March 2019, 020050 pp. 1-6.
15. Krason W, Bogusz P. Strain research of side joints of floating bridge in lab bending test, Experimental Mechanics of Solids Materials Research Proceedings 12. 2019:96-103, Materials Research Forum LLC. https://doi.org/10.21741/9781644900215-14
16. Krason W, Bogusz P, Popławski A, Stankiewicz M. Selected aspects of stand tests of the floating prototype bridge connector. Experimental Mechanics of Solids Materials Research Proceedings 12. 2019:90-95. Materials Research Forum LLC. https://doi.org/ 10.21741/9781644900215-13
17. NO-54-A203: Mosty składane. Wymagania ogólne. http://g.ekspert.infor.pl/p/_dane/akty_pdf/U23/2001/22/186.pdf
18. Krason W, Kozłowski R, Derewońko A, Golczak K. Selected Aspects of Simulation of Multi-Module Mechanisms with the Use of Multibody Method. Journal of KONES.2012;19(1):207-214 DOI: 10.5604/12314005.1137359
19. EP2570551B1. A cassette of a floating bridge. 2012. Military University of Technology.
20. Zienkiewicz OC, Taylor L, Zhu JZ. The Finite Element Method: Its Basis and Fundamentals. Elsevier Butterworth-Heinemann. Berlin 2005.
21. Fengzong Gong, Fei Han, Yingjie Wang, Ye Xia. Bridge Damping Extraction Method from Vehicle–Bridge Interaction System Using Double-Beam Mode. Appl. Sci. 2021;11(21): 10304. https://doi.org/10.3390/app112110304
22. Lixia Peng, Zhiqiang Gao, Zhaoyang Ban, Feng Gao, Weiping Fu. Dynamic Tangential Contact Stiffness and Damping Model of the Solid–Liquid Interface. Machines.2022;10:804. https://doi.org/10.3390/machines10090804

This research was funded by the MILITARY UNIVERSITY OF TECHNOLOGY, grant number PBS 23-937/WAT/2018, and the APC was funded by the Ministry of Science and Higher Education of Poland.

Agnieszka Derewońko: https://orcid.org/0000-0002-6050-6359

Wiesław Krasoń: https://orcid.org/0000-0001-7242-648X